Available online at www.sciencedirect.com
SCIENCE DIRECT
Journal of the European Ceramic Society 26 (2006) 1301–1309
www.elsevier.com/locate/jeurceramsoc

Characterization of different starch types for their application in ceramic processing

Eva Gregorová [a,*], Willi Pabst [a], Ivan Bohačenko [b]

[a] *Department of Glass and Ceramics, Institute of Chemical Technology in Prague, Technická 5, 166 28 Prague 6, Czech Republic*
[b] *Food Research Institute Prague, Radiová 7, 102 31 Prague 10, Czech Republic*

Received 24 November 2004; received in revised form 17 February 2005; accepted 25 February 2005
Available online 13 May 2005

Abstract

Starch is a frequently used pore-forming agent in ceramic technology. Moreover, it can take over the function of a body-forming agent in a recently developed process, called starch consolidation casting. Upon firing the starch polymers are burnt out without residues and leave a pore structure determined by the type of starch applied. In this paper, five commonly available starch types (potato, wheat, tapioca, corn and rice starch) are characterized with respect to size and shape. Size distributions are measured via laser diffraction and microscopic image analysis. Rice starch is found to be the smallest type (median size 4.4–4.8 μm), potato starch the largest (median size 46–49 μm) and the other types intermediate (median size 12–21 μm). The distribution is narrow for corn and tapioca starch (span approximately 1.1), while potato, wheat and rice starch are relatively polydisperse (span approximately 1.35–1.65). The shape of the starch granules is most anisometric for potato starch (average aspect ratio 1.3–1.4). All other starch types, although possibly of polyhedral shape (tapioca, corn and rice starch), are more isometric, i.e. very close to an average aspect ratio of 1.

Keywords: Starch consolidation casting; Microstructure—prefiring/final; Optical microscopy; Porosity

1. Introduction

Starch is one of the frequently used pore-forming agents in ceramic technology.[1,2] Due to its chemical composition (a polysaccharide consisting essentially of C, H and O only) this natural biopolymer is easily burnt out during firing without residues in the final ceramic body. In a recently developed process, called starch consolidation casting (SCC), starch can additionally take the role of a body-forming agent.[3–9] This process exploits the ability of starch granules to swell in aqueous media at elevated temperature and enables ceramic green bodies to be formed from starch-containing aqueous ceramic suspensions by casting into non-porous molds (e.g. polymer or metal molds). Principles, processing details and modeling issues concerning the SCC process as well as microstructure–property characterization of final ceramics prepared by SCC can be found in Refs. 10–15. Of course, also the SCC process results in porous ceramics with a microstructure determined by the type of starch used. However, optimization of the SCC process is a highly complex task, which is complicated by the intricate time–temperature behavior of starch in aqueous media and the non-equilibrium nature of phase transitions (e.g. gelatinization and retrogradation).[16,17] Although starch granules can generally change their size (and volume) and possibly shape during swelling, the initial size and shape will determine the characteristics of the pore space of the final ceramics to a large degree.

In any case, as a first step towards efficient microstructural control by the SCC process, it is necessary to know the initial size, shape and size distribution of the starch type used. In particular, concerning size distribution, it is desirable to dispose of a characterization in terms of laser diffraction (LD) data and in terms of microscopic image analysis (MIA) data. The former (LD) is a convenient modern standard method that can be routinely applied in process optimization and produc-

* Corresponding author.
E-mail address: gregoroe@vscht.cz (E. Gregorová).

0955-2219/$ – see front matter © 2005 Elsevier Ltd. All rights reserved.
doi:10.1016/j.jeurceramsoc.2005.02.015

tion control, while the latter (MIA) is a method that can be conveniently applied for the characterization of fired ceramic bodies. In other words, only by MIA it is possible to relate the particle size distribution of the pore-forming agent directly to the pore size distribution in the fired ceramics. In spite of the immense literature on starch science and technology, it seems that a systematic comparison between LD data and MIA data from the viewpoint of particle statistics is not available. The purpose of this paper to provide such a comparison and to present the individual characteristics for five native starch types which are commercially available in the world market: potato, wheat, tapioca, corn and rice.

The size and shape information provided in this paper should be helpful to realistically delimit the potential microstructural goals that can be attacked with starch as a pore-forming agent (in conventional ceramic shaping technologies or in the SCC process) and may serve as a guideline in selecting the appropriate starch type for a concrete application in mind. The comparison between LD and MIA results is a necessary precondition for future process optimization and improved microstructural control.

2. Starch types

Starches are complex biopolymers of natural origin, occurring in the form of granules in plant tissue. Chemically, they consist essentially of two types of polysaccharides (glucose polymers), amylose and amylopectin, cf. Table 1. For a detailed characterization of composition, structure and properties of starch, including the time–temperature behavior in aqueous media (with or without additional solutes), the reader can refer to several excellent reviews.[18–20] What is of primary interest in the present paper is the size and shape characterization of native (i.e. unmodified) starch granules in the unswollen state, which is the initial state used for mixing into ceramic suspensions and is related to the pore structure, resulting in the final ceramic after starch burnout, cf. Figs. 1 and 2 and similar micrographs, e.g. in Ref. 1. It has to be emphasized of course that the pore size distribution need by no means be identical to the initial size distribution of the starch granules. Depending on the processing conditions, a possible influence of starch swelling on the final pore size has to be taken into account, although the choice of the adequate starch type will always be the primary and most important step for pore size control. In this sense, Figs. 1 and 2 should

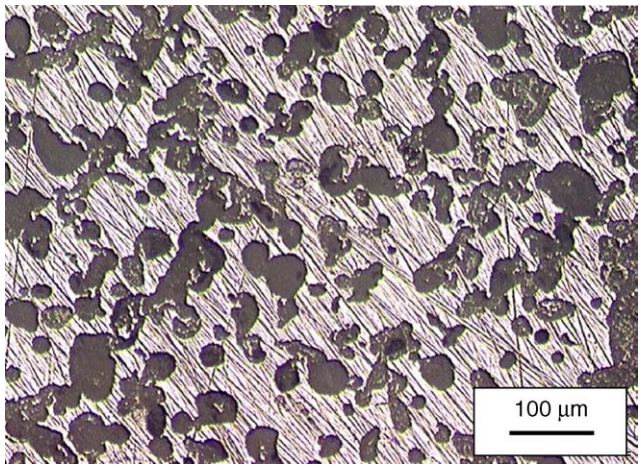

Fig. 1. Optical micrograph of zirconia ceramics prepared by SCC from a suspension containing 30 vol.% (based on solids) of potato starch.

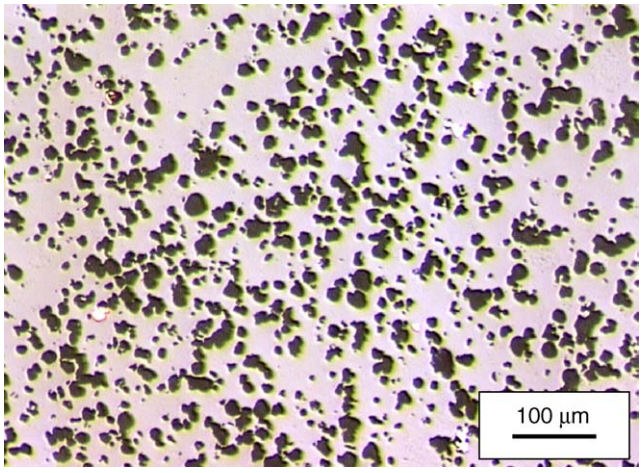

Fig. 2. Optical micrograph of zirconia ceramics prepared by SCC from a suspension containing 15 vol.% (based on solids) of corn starch.

be viewed as paradigmatic examples. They show zirconia ceramics prepared from 72 wt.% zirconia suspensions (TZ-3YE, Tosoh, Japan) after mixing at room temperature with 30 vol.% potato starch and 15 vol.% corn starch (based on solids), respectively. After casting into metal molds, heating at 80 °C for 2 h, demolding and drying at 105 °C for 12 h the ceramics were fired at 1400 °C (heating rate 1 °C/min below 600 °C and 2 °C/min above 600 °C, dwell 2 h), resulting in total porosities of 31.5 and 20%, respectively. Although the two starch types exhibit distinctly different processing

Table 1
Characteristics of starch types (typical values for orientational purposes), including the rate of granular swelling and the temperature range for gelatinization in excess water[17,19]

Starch type	Amylose content (%)	Amylopectin content (%)	Rate of granular swelling	Gelatinization start (°C)	Gelatinization end (°C)
Potato	20–21	79–80	Fast	50–56	68
Wheat	25–30	70–75	Slower	58	64
Tapioca	16–17	83–84	Fast	49	65
Corn	25–28	72–75	Slower	62	72–80
Rice	17–30	70–83	Slower	58–69	79–86

behavior and controllability, it is evident that the difference in pore size is primarily a consequence of the difference in the initial granule size of potato starch and corn starch.

Being of natural origin, it is clear that all product characteristics of native starch, including size and shape, exhibit a relatively broad variance, depending on genetic type of the plants, breeding and growth conditions (climate, sunshine, humidity), extraction procedure and batch-to-batch variations. Potato (*Solanum tuberosum*) and tapioca starches are tuber or root starches, the latter obtained from the cassava plant (*Manihot esculenta*), while wheat, corn and rice starch are cereal starches (from *Triticum vulgare*, *Zea mays* L. and *Oryza sativa* L., respectively).

All five starch types investigated here are commercially available from several producers on the world market. In Europe, potato, corn and wheat starch are the most common types. The samples for the present investigation were potato starch Solamyl (Natura a.s., Czech Republic), corn starch Gustin (Dr. Oetker a.s., Czech Republic) and wheat starch from Amylon a.s., Czech Republic. Rice and tapioca starch, currently less common in Europe, were test samples provided by the Vyzkumný ústav potravinářský Praha (VUPP), Czech Republic.

3. Measurement details and evaluation procedure

All five starch types (potato, tapioca, wheat, corn, and rice) have been characterized by LD and MIA. The reader can refer to standard monographs[21,22] for measurement principles of these methods. Laser diffraction was carried out in a standard way[23,24] on the particle sizer Analysette 22 (Fritsch Laborgeratebau GmbH, Germany) using a He–Ne laser (wavelength approximately 0.6 μm) and performing a model-independent evaluation via Fraunhofer theory. No sample preparation was necessary prior to measurement, since complete dispersion can be achieved just by applying ultrasound during measurement itself. For microscopic image analysis the starch granules were dispersed in distilled water at room temperature, dropped on an object slide and dried in air at room temperature. A number of micrographs was made of each starch type with an optical microscope Jenapol (Zeiss, Germany) and a commercial image analyzing software package (LUCIA G, version 4.81, Laboratory Imaging, Czech Republic) was used for data recording. Table 2 includes the number of objects (starch granules) counted for the individual starch types in the present investigation.

With the help of the image analysis software individual starch granules were circumscribed manually by simple well-defined equivalent area objects (circles or ellipses). From the area (measured by pixel counting in the image analysis software) a projected area diameter, i.e. the diameter of a circle equivalent (with respect to area) to the projected particle outline, is automatically calculated. In the case of wheat, tapioca, corn and rice the marking could be done with circles, due to their isometric shape (Figs. 4–7). However, for potato starch, cf. Fig. 3 (obviously the most anisometric of the starch types investigated in this paper), it appeared useful to use equivalent ellipses (five-point ellipses) for marking. This enables one to quantify shape information via an aspect ratio (i.e. the ratio between maximum and minimum Feret diameter), in addition to the size information contained in the projected area diameter.

The primary results of MIA are number-weighted size distributions in the form of so-called frequency histograms (q_0). In order to compare these results with the LD results, which are volume-weighted size distributions (q_3), it is necessary to transform the MIA results (so-called "q_0–q_3 transformation", cf. Ref. 23). For isometric particles or systems with a size-invariant aspect ratio this can be done very easily by replacing the number of objects N_i counted in a certain size class D_i by the quantity $N_i D_i^3$. The corresponding cumulative size distributions (Q_3) are easily obtained by stepwise summation of the frequency histograms and normalization to 100%, cf. Refs. 21–23.

4. Results and discussion

Figs. 3–7 show micrographs of potato, wheat, tapioca, corn and rice starch, respectively. It is evident that potato starch exhibits the largest and most anisometric granules (Fig. 3). The deviation from sphericity is clearly towards prolate shapes. Polydispersity is a common feature of all starch types, but wheat starch shows a large amount of small grains beside many large grains, while intermediate sizes are apparently missing (Fig. 4). Most wheat starch granules seem to be spherical, although some of the larger grains might be of slightly oblate shape, corresponding to the lenticular granules described in the starch literature.[17–20] Tapioca and corn starch (Figs. 5 and 6) appear very similar to each other with

Table 2
Number of objects counted via MIA for the respective starch types and characteristic measures of the volume-weighted particle size distributions (MIA: microscopic image analysis, LD: laser diffraction)

Starch type	Number of objects counted	Median (MIA) (μm)	Mode (MIA) (μm)	Median (LD) (μm)	Mode (LD) (μm)	Span (LD)
Potato	1600	46.3	56	49.0	54.9	1.45
Wheat	3315	20.7	22.5	20.0	22.7	1.65
Tapioca	4173	12.2	15	13.5	15.0	1.07
Corn	4204	12.9	15	14.2	14.8	1.13
Rice	4083	4.8	5.2	4.4	5.2	1.35

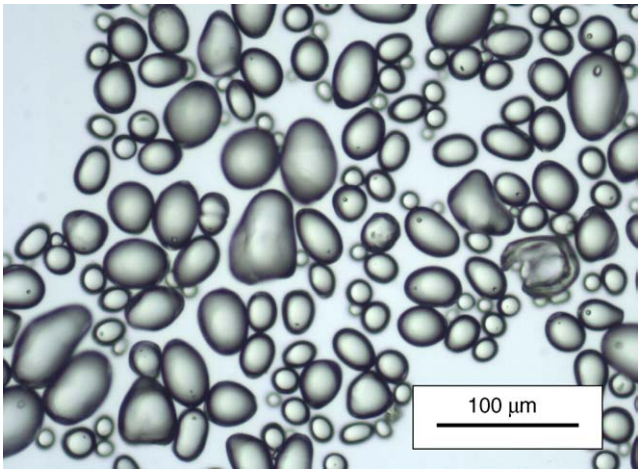

Fig. 3. Optical micrograph of native potato starch.

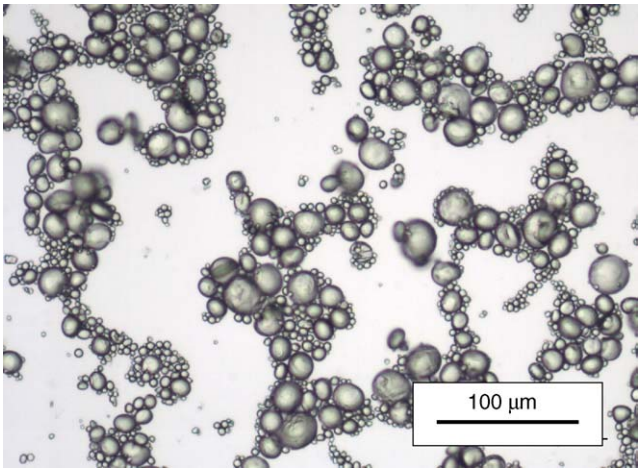

Fig. 4. Optical micrograph of native wheat starch.

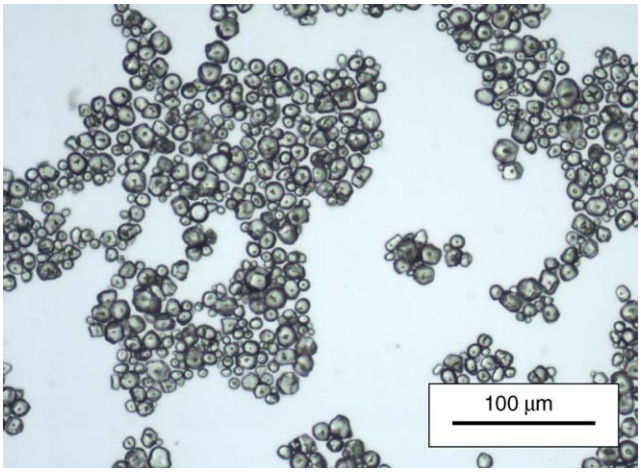

Fig. 5. Optical micrograph of native tapioca starch.

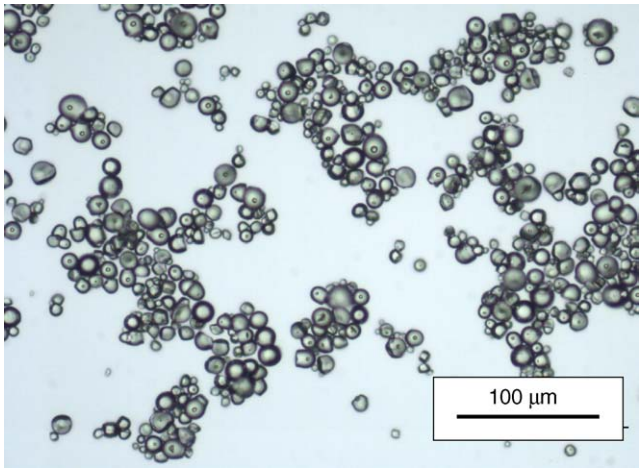

Fig. 6. Optical micrograph of native corn starch.

respect to size (evidently smaller than potato starch and the large size fraction of wheat starch), while rice starch (Fig. 7) is definitely the smallest of all. The shape of tapioca, corn and rice starch is isometric but often non-spherical (polyhedral). All these qualitative findings are in agreement with what is known from the starch literature.[16–20]

In order to quantify the statements just made, it is necessary to consider the measured size distributions. Fig. 8 shows the number-weighted size distribution q_0 (frequency histogram) of potato starch determined by MIA, while Fig. 9 shows the same data after q_0–q_3 transformation, i.e. in terms of relative volume instead of number. In the present case, the q_0–q_3 transformation could be simplified as described above, since the average aspect ratio is approximately size-invariant (total grand arithmetic mean of the invidual size class arithmetic means: 1.41 ± 0.09), cf. Fig. 10. Note, however, that this does not imply that all grains are of the same shape (cf. Fig. 3). On the contrary, similar to the individual size classes the system as a whole exhibits an aspect ratio distribution, cf. Fig. 11. For the potato starch investigated here, this

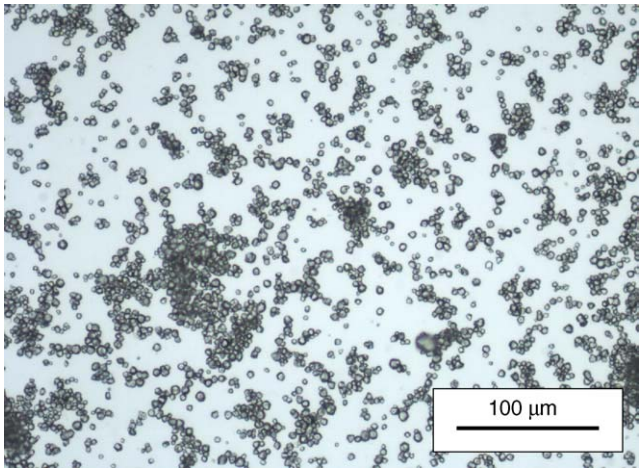

Fig. 7. Optical micrograph of native rice starch.

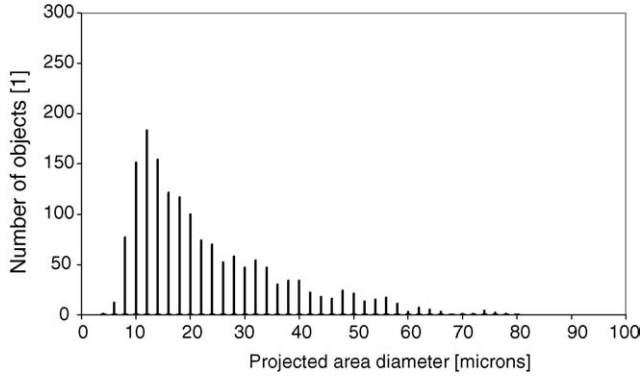

Fig. 8. Number-weighted frequency histogram (q_0) of potato starch determined by MIA.

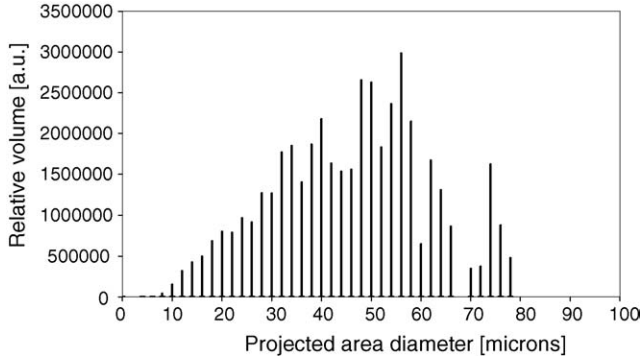

Fig. 9. Volume-weighted size distribution (q_3) of potato starch (obtained from the MIA data in Fig. 8 via q_0–q_3 transformation under the assumption of a size-invariant aspect ratio).

distribution can be characterized by a mode of 1.25, a median of 1.25 and an arithmetic mean of 1.35 ± 0.22. According to all these shape measures potato starch exhibits a small degree of anisometry. Evidently, all other starch types are more isometric.

Fig. 12 shows the volume-weighted size distributions (q_3) of potato starch determined from MIA (after q_0–q_3 transformation) in comparison with the results of LD, in the usual representation with logarithmic abscissa. Fig. 13 shows

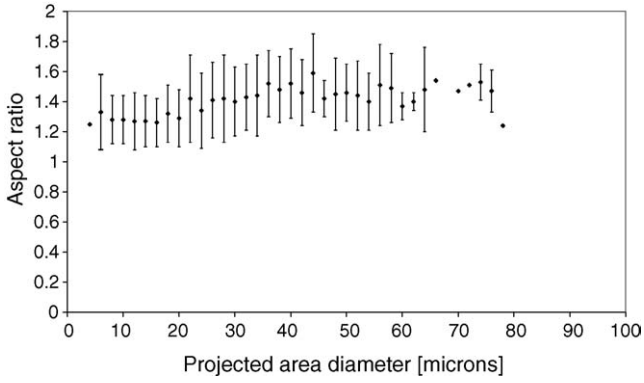

Fig. 10. Size dependence of the aspect ratio of potato starch granules (arithmetic mean: 1.41 ± 0.09).

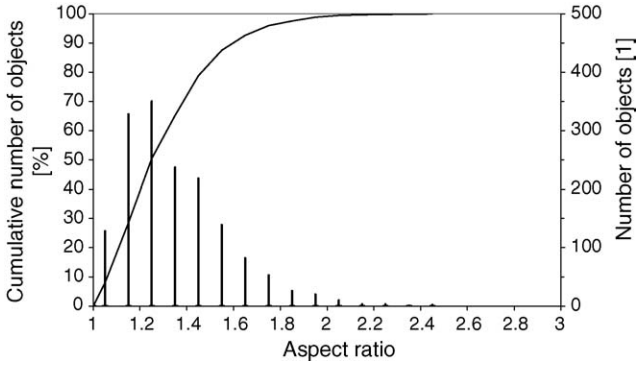

Fig. 11. Aspect ratio distribution (cumulative curve—left ordinate, frequency histogram—right ordinate) of potato starch granules (median: 1.25, mode: 1.25, arithmetic mean: 1.35 ± 0.22).

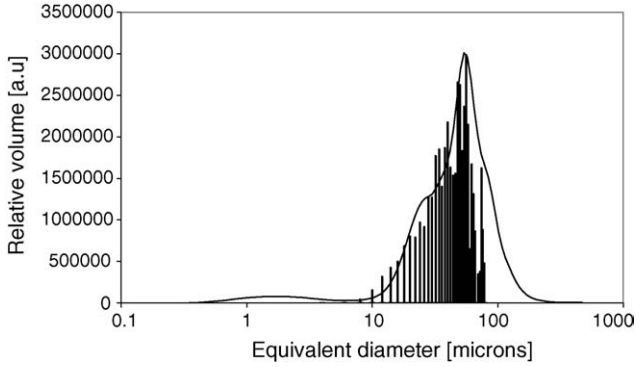

Fig. 12. Volume-weighted size distributions of potato starch (q_3 histogram obtained from the MIA data via q_0–q_3 transformation, cf. Fig. 9; curve measured by LD).

the corresponding cumulative curves (dashed curve: MIA, solid curve: LD). Figs. 14, 17, 20 and 23 show the number-weighted size distributions (MIA, q_0), Figs. 15, 18, 21 and 24 show the volume-weighted size distributions (MIA and LD, q_3) and Figs. 16, 19, 22 and 25 the corresponding cumulative curves (MIA and LD, Q_3) of wheat, tapioca, corn and rice starch, respectively. A striking feature is the unusual shape of the q_0 histogram for wheat starch: the small size mode (size class 3.5–5.5 μm) is extremely high, i.e. high enough to

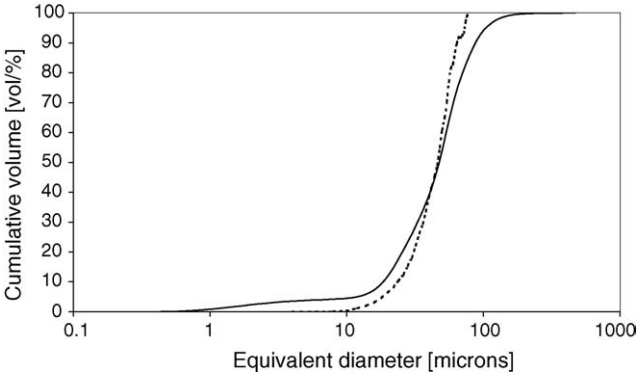

Fig. 13. Volume-weighted size distributions of potato starch (Q_3 cumulative curves; dotted—MIA, solid—LD).

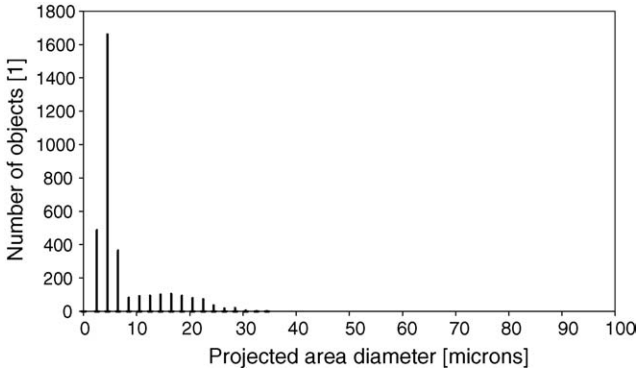

Fig. 14. Number-weighted frequency histogram (q_0) of wheat starch determined by MIA.

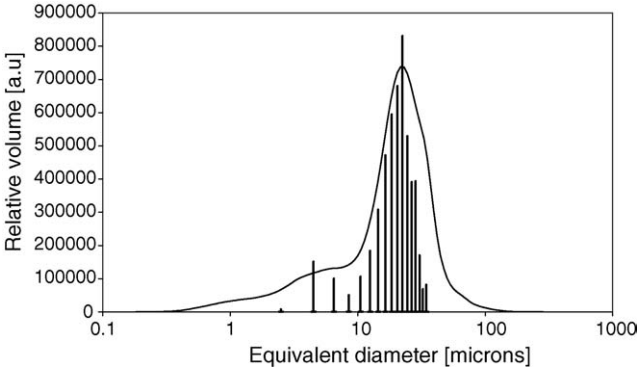

Fig. 15. Volume-weighted size distributions of wheat starch (q_3 histogram obtained from the MIA data via q_0–q_3 transformation, cf. Fig. 14; curve measured by LD).

be retained even after q_0–q_3 transformation. This is characteristic for the bimodal nature of wheat starch mentioned in the starch literature.[17,20] Comparing MIA and LD results the following conclusions can be made:

1. For all five starch types investigated in this work the agreement between MIA results (after q_0–q_3 transformation) and LD results is generally satisfactory in the central region of the size distributions. It is evident from Table 2 that the median values of the MIA and LD size distributions are very close and that the mode values are in excellent agreement.
2. In the small-size region (particularly around 1–2 μm) LD generally seems to overestimate the content of fines. Although it may be argued that in this size region the evaluation of LD results via Fraunhofer theory is inappropriate (and Mie theory should be used[21,22,24]), it is highly probable that the LD results are nevertheless the more reliable ones, because with MIA the size and number of such small particles is seriously affected by the resolution limit of

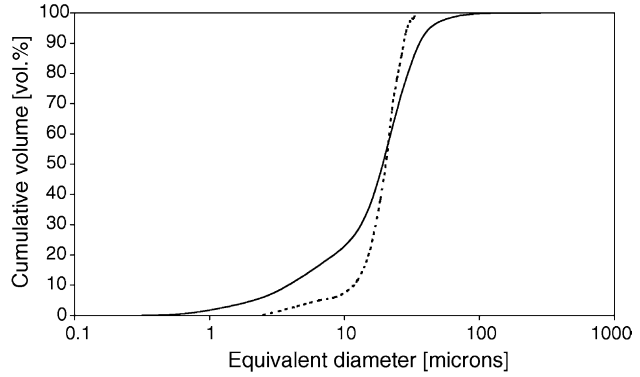

Fig. 16. Volume-weighted size distributions of wheat starch (Q_3 cumulative curves; dotted—MIA, solid—LD).

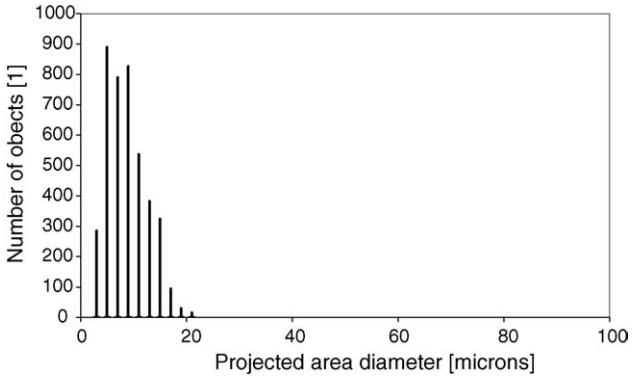

Fig. 17. Number-weighted frequency histogram (q_0) of tapioca starch determined by MIA.

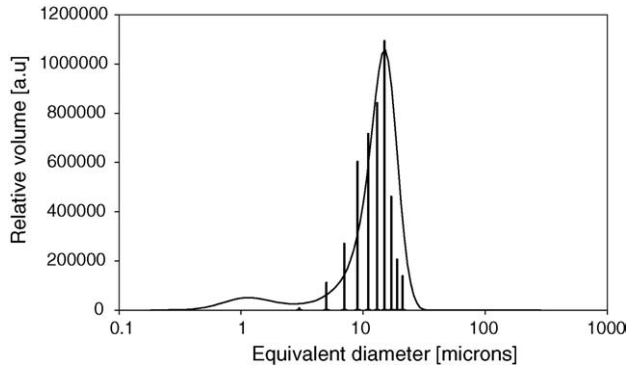

Fig. 18. Volume-weighted size distributions of tapioca starch (q_3 histogram obtained from the MIA data via q_0–q_3 transformation, cf. Fig. 17; curve measured by LD).

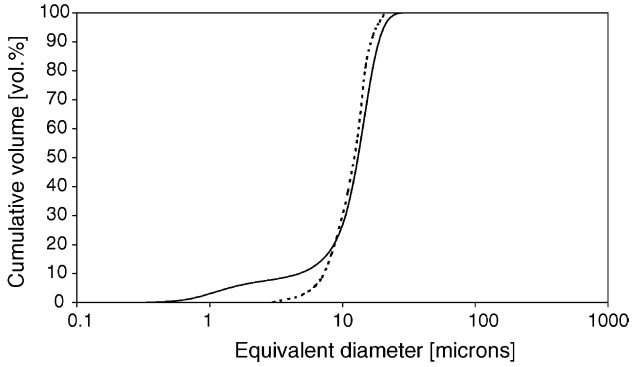

Fig. 19. Volume-weighted size distributions of tapioca starch (Q_3 cumulative curves; dotted—MIA, solid—LD).

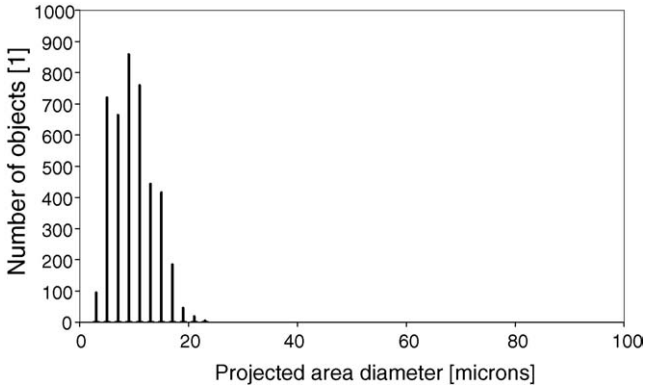

Fig. 20. Number-weighted frequency histogram (q_0) of corn starch determined by MIA.

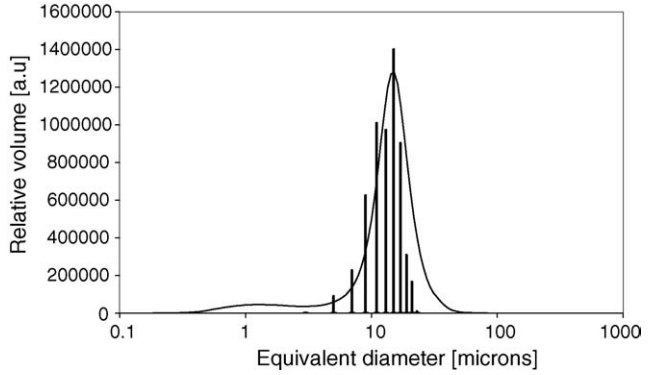

Fig. 21. Volume-weighted size distributions of corn starch (q_3 histogram obtained from the MIA data via q_0–q_3 transformation, cf. Fig. 20; curve measured by LD).

light-optical microscopes: if the particles are detected at all, the size values in this region are strongly distorted by interference phenomena near the resolution limit.[21]

3. In the large-size region the LD results generally extend to higher size values than the MIA results. Again, there is a strong argument in favor of the LD results: the number of particles is considerably larger and thus the statistics is more reliable. Even a comparatively small number of large particles, if statistically relevant, will have a visible influence on the volume-weighted size distribution (q_3 or Q_3) determined by LD, while it may remain undetected by MIA and meaningless in a number-weighted size distribution (q_0 or Q_0).
4. Potato starch is the largest starch type with a median equivalent diameter (D_{50}) between 46.3 μm (MIA) and 49 μm (LD), rice starch the smallest with D_{50} between 4.8 μm (MIA) and 4.4 μm (LD). An appropriate measure of the

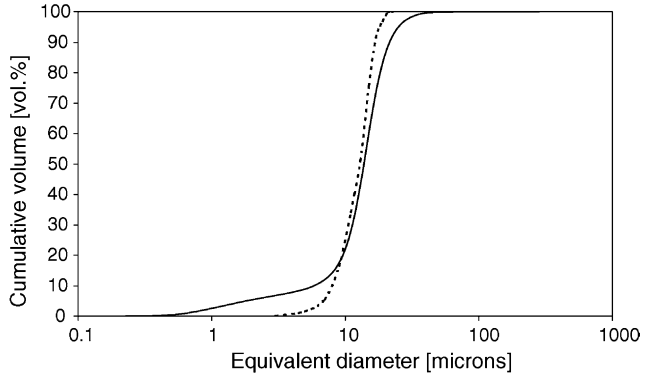

Fig. 22. Volume-weighted size distributions of corn starch (Q_3 cumulative curves; dotted—MIA, solid—LD).

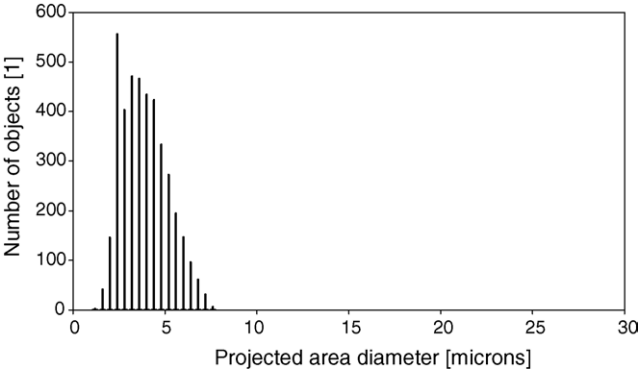

Fig. 23. Number-weighted frequency histogram (q_0) of rice starch determined by MIA.

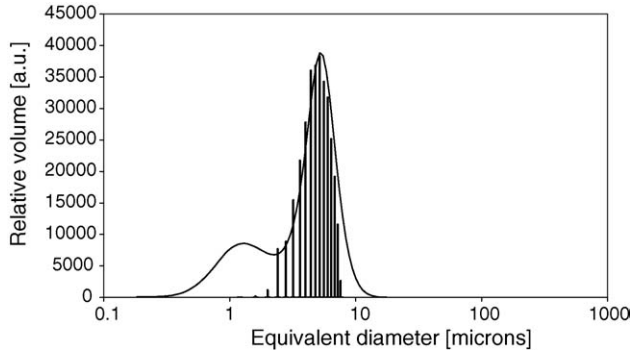

Fig. 24. Volume-weighted size distributions of rice starch (q_3 histogram obtained from the MIA data via q_0–q_3 transformation, cf. Fig. 23; curve measured by LD).

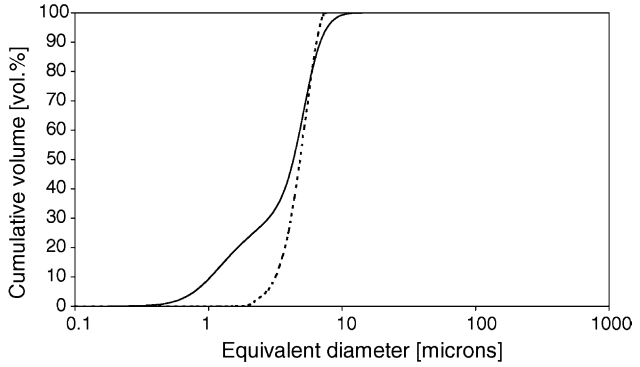

Fig. 25. Volume-weighted size distributions of rice starch (Q_3 cumulative curves; dotted—MIA, solid—LD).

width of the distribution is the so-called span defined as

$$\text{span} = \frac{D_{90} - D_{10}}{D_{50}},$$

where D_{90} is the 90% and D_{10} the 10% undersize quantile. The span values of the LD Q_3 distributions in Table 2 indicate that tapioca and corn starch, apart from being of almost the same size and shape, are both relatively monodisperse (span 1.07–1.13), while rice, potato and especially wheat starch are much more polydisperse (span 1.35–1.65).

Although it clearly follows that for the characterization of native starch LD is a more efficient method than MIA and will usually be preferred in routine measurements, the above comparison between MIA and LD results is of fundamental importance in ceramic science and technology, since the attempt to produce ceramics with controlled microstructure (porosity, pore and pore space characteristics) requires a comparison between the size distribution of the pore-forming agents and the size distribution of the pores in the final ceramic body. Routinely (i.e. when tomographic 3D techniques[25–27] are to be avoided), the latter can be determined in two ways: either by mercury intrusion or by microscopic image analysis of 2D polished sections. Both ways are not without drawbacks: in the first the oversimplified and unrealistic cylindrical tube model is usually exploited to express the results in terms of equivalent pore diameters,[21,28] while the results of the latter are distorted by the fact that the pores are cutted statistically in random planes not corresponding to the true (i.e. maximum) pore diameter. Nevertheless, the latter problem (so-called Wicksell's corpuscle problem) can for many practical cases be solved using the so-called Saltykov transformation,[29–31] while the mercury intrusion results must necessarily remain unrealistic for pores formed with spherical pore-forming agents. However, based on the findings of MIA it was possible to assign the minimum in the pore size distribution measured by mercury intrusion to the average size of the pore throats, i.e. the interconnecting channels between overlapping spherical pores.[10]

Based on the findings of this paper it can now be considered as justified using laser diffraction for the characterization of the pore-forming agent (starch granules) and compare these results directly with the pore-size distribution of the final ceramic bodies (resulting after starch burnout during firing) measured by microscopic image analysis. In particular, the median and mode values of the size distributions can be expected to be quite reliable, when the number of objects (pores) counted is not much less than in the present investigation. We note, however, that this comparison is only possible due to the sufficiently isometric shape of the starch granules and cannot be generalized to other, more anisometric, pore-forming agents.

It is known from sintering theory[32] that when large pores are present in a fine-grained ceramic green body, these large pores do not exhibit significant shrinkage, since they are thermodynamically stable or even show a tendency to grow.[33] Thus, when starch granules are used as a pore-forming agent in traditional ceramic processing (slip casting, extrusion, pressing) the pores resulting from the pore-forming agent (burnt out during firing) can be expected to be of approximately the same size as the initial starch granule size. Surprisingly, preliminary microstructural studies with ceramics prepared by starch consolidation casting (SCC), where starch is a pore-forming and a body-forming (swelling) agent at the same time, seem to indicate that also in this process the swelling potential of starch is by no means fully exploited (at least for potato starch where swelling can be extremely large) and the resulting pore size distribution is not too much different from the initial size distribution of the starch granules. The connection between swelling kinetics, rheological changes and body formation in the SCC process, questions of starch burnout and sintering as well as microstructure–property relations in ceramics prepared by SCC will be adressed in more detail in forthcoming papers.

5. Summary and conclusions

Five starch types, all commercially available on the world market, have been characterized with respect to size and shape. Size distributions have been measured by LD and MIA. The latter, although much more operator-intensive and time-consuming, was necessary in order to verify the possibility to replace MIA by LD in routine measurements and to justify the future use of LD (and not MIA) results for a direct comparison with resulting pore-size distributions measured by MIA. In particular, good agreement was found for the central region of the size distributions and therefore the use of median and/or mode values for system characterization can be recommended. This result should be valid for all approximately isometric objects and is not related to any specific starch type. We emphasize, however, that for strongly anisometric pore-forming agents agreement of MIA and LD results cannot be expected and thus in general it is not possible to replace the MIA measurement by a LD measurement.

Concerning the potential use as pore-forming agents in ceramic technology or as combined pore-and-body-forming agents in the SCC process the following can be said: Notwithstanding the fact that all starches are natural biopolymers (which naturally implies a relatively large scatter of size and shape characteristics and doubtlessly sets certain limits to the precision of microstructural control achievable in principle), a comparison with the information available in the extensive starch literature shows that the principal differences revealed in this paper can be considered as quite generally valid for native starch and the values as typical for the respective starch types. Rice starch is the smallest, potato starch the largest of the easily available starch types (with median sizes of 4–5 μm and 45–50 μm, respectively). Wheat starch is intermediate ($D_{50} \approx 20$ μm) and exhibits a strongly bimodal size distribution, which might be exploitable for achieving

extremely high porosities (fractal or "Appolonian" packing of pores). Tapioca and corn starch exhibit very similar size and shape characteristics ($D_{50} \approx 12$–$14\,\mu m$) and a relatively narrow size distribution (span ≈ 1.1, compared to values between 1.35 and 1.65 for the other three starch types). Thus, from the viewpoint of pore size control it should be possible to replace tapioca starch by corn starch and vice versa. Nevertheless, other characteristics can be very different, e.g. the swelling behavior and the gelatinization temperature range listed in Table 1. Potato starch is the most anisometric of the starch types investigated (average aspect ratio ≈ 1.3–1.4). All other starch types, although possibly of polyhedral shape (tapioca, corn and rice starch), are more isometric, i.e. very close to an average aspect ratio of 1.

Acknowledgement

This work was part of the project "Preparation and properties of advanced materials—modelling, characterization, technology", supported by the Czech Ministry of Education, Youth and Sports (Grant No. MSM 223100002). The support is gratefully acknowledged.

References

1. Díaz, A. and Hampshire, S., Characterization of porous silicon nitride materials produced with starch. *J. Eur. Ceram. Soc.*, 2004, **24**, 413–419.
2. Reynaud, C., Thévenot, F., Chartier, T. and Besson, J.-L., Mechanical properties and mechanical behaviour of SiC dense-porous laminates. *J. Eur. Ceram. Soc.*, 2005, **25**, 589–597.
3. Lyckfeldt, O. and Ferreira, J. M. F., Processing of porous ceramics by "starch consolidation". *J. Eur. Ceram. Soc.*, 1998, **18**, 131–140.
4. Alves, H. M., Tarí, G., Fonseca, A. T. and Ferreira, J. M. F., Processing of porous cordierite bodies by starch consolidation. *Mater. Res. Bull.*, 1998, **33**, 1439–1448.
5. Lyckfeldt, O., Novel water-based shaping of ceramic components. *Br. Ceram. Proc.*, 1999, **60**, 219–220.
6. Lemos, A. F. and Ferreira, J. M. F., Porous bioactive calcium carbonate implants processed by starch consolidation. *Mater. Sci. Eng.*, 2000, **C11**, 35.
7. Bowden, M. E. and Rippey, M. S., Porous ceramics formed using starch consolidation. *Key Eng. Mater.*, 2002, **206–213**, 1957–1960.
8. Týnová, E., *Alumina Ceramics Prepared by Casting with Organic Additives*. MSc thesis, ICT Prague, Prague, 2000 (in Czech).
9. Týnová, E., New trends in shaping of ceramics (in Czech). *Sklář a keramik*, 2003, **53**, 209–211.
10. Pabst, W., Gregorová, E., Havrda, J. and Týnová, E., Gelatin casting and starch consolidation of alumina ceramics. In *Ceramic Materials and Components for Engines*, ed. J. G. Heinrich and F. Aldinger. Wiley-VCH, Weinheim, 2001, pp. 587–592.
11. Týnová, E., Pabst, W., Gregorová, E. and Havrda, J., Starch consolidation casting of alumina ceramics—body formation and microstructural characterization. *Key Eng. Mater.*, 2002, **206–213**, 1969–1972.
12. Pabst, W., Týnová, E., Mikač, J., Gregorová, E. and Havrda, J., A model for the body formation in starch consolidation casting. *J. Mater. Sci. Lett.*, 2002, **21**, 1101–1103.
13. Týnová, E., Pabst, W., Gregorová, E. and Havrda, J., Zirconia and alumina-zirconia composites ceramics prepared by starch consolidation. In *Proceedings of the Second International Conference on Shaping of Advanced Ceramics*, ed. J. Luyten and J. P. Erauw. Vito, Mol, 2002, pp. 77–82.
14. Týnová, E., Gregorová, E., Pabst, W. and Černý, M., Influence of the starch type on microstructure and properties of oxide ceramics prepared by starch consolidation (in Czech). In *Proceedings of the Fifth Conference on Preparation of Ceramic Materials*, ed. B. Plešingerová and T. Kuffa. Technical University in Košice, Košice, 2003, pp. 81–85.
15. Týnová, E., Pabst, W. and Mikač, J., Starch swelling and its role in modern ceramic shaping technology. *Macromol. Symp.*, 2003, **203**, 295–300.
16. Jackson, D. S., Starch: functional properties. In *Encyclopaedia of Food Science, Food Technology, and Nutrition*, ed. R. Macrae, R. K. Robinson and M. J. Sadler. Academic Press, London, 1993, pp. 4377–4381.
17. Biliaderis, C. G., Structures and phase transitions of starch polymers. In *Polysaccharide Association Structures in Food*, ed. R. H. Walter. Marcel Dekker, New York, 1998, pp. 57–168.
18. Zobel, H. F. and Stephen, A. M., Starch: structure, analysis, and application. In *Food Polysaccharides and Their Applications*, ed. A. M. Stephen. Marcel Dekker, New York, 1995, pp. 19–66.
19. Daniel, J. R. and Whistler, R. L., Starch: sources and processing. In *Encyclopaedia of Food Science, Food Technology, and Nutrition*, ed. R. Macrae, R. K. Robinson and M. J. Sadler. Academic Press, London, 1993, pp. 4377–4380.
20. Jackson, D. S., Starch: structure, properties and determination. In *Encyclopaedia of Food Science, Food Technology, and Nutrition*, ed. R. Macrae, R. K. Robinson and M. J. Sadler. Academic Press, London, 1993, pp. 4372–4377.
21. Allen, T., *Particle Size Measurement, Vols 1 and 2* (*5th ed.*). Chapman & Hall, London, 1997.
22. Xu, R., *Particle Characterization: Light Scattering Methods*. Kluwer Academic Publishers, Dordrecht, 2000.
23. Pabst, W., Berthold, C. and Gregorová, E., Size and shape characterization of polydisperse short fiber systems. *J. Eur. Ceram. Soc.*, 2006, **26**, 1121–1130.
24. Pabst, W., Kuneš, K., Havrda, J. and Gregorová, E., A note on particle size analyses of kaolins and clays. *J. Eur. Ceram. Soc.*, 2000, **20**, 1429–1437.
25. Arns, C. H., Knackstedt, M. A. and Mecke, K. R., Characterising the morphology of disordered materials. In *Morphology of Condensed Matter*, ed. K. Mecke and D. Stoyan. Springer-Verlag, Berlin, 2002, pp. 37–74.
26. Vogel, H.-J., Topological characterization of porous media. In *Morphology of Condensed Matter*, ed. K. Mecke and D. Stoyan. Springer-Verlag, Berlin, 2002, pp. 75–92.
27. Magerle, R., Nanotomography: real-space volume imaging with scanning probe microscopy. In *Morphology of Condensed Matter*, ed. K. Mecke and D. Stoyan. Springer-Verlag, Berlin, 2002, pp. 93–106.
28. Gregg, S. J. and Sing, K. S. W., *Adsorption, Surface Area and Porosity* (*2nd ed.*). Academic Press, London, 1982.
29. Saltykov, S. A., *Stereographische Metallographie*. VEB Deutscher Verlag fur Grundstoffindustrie, Leipzig, 1974.
30. Russ, J. C. and Dehoff, R. T., *Practical Stereology* (*2nd ed.*). Kluwer Acedemic Publishers Academic Press, New York, 2000.
31. Ohser, J. and Mucklich, F., *Statistical Analysis of Microstructures in Materials Science*. Wiley, Chichester, 2000.
32. German, R. M., *Sintering Theory and Practice*. John Wiley & Sons, New York, 1996.
33. Shi, J. L., Solid state sintering of ceramics: pore microstructure models, densification equations and applications. *J. Mater. Sci.*, 1999, **34**, 3801–3812.